



HAL
open science

Synthesis and magnetic properties of size-selected CoPt nanoparticles

F Tournus, N Blanc, A Tamion, M Hillenkamp, Véronique Dupuis

► **To cite this version:**

F Tournus, N Blanc, A Tamion, M Hillenkamp, Véronique Dupuis. Synthesis and magnetic properties of size-selected CoPt nanoparticles. *Journal of Magnetism and Magnetic Materials*, 2011, 323, pp.1868 - 1872. 10.1016/j.jmmm.2011.02.024 . hal-04082766

HAL Id: hal-04082766

<https://hal.science/hal-04082766>

Submitted on 26 Apr 2023

HAL is a multi-disciplinary open access archive for the deposit and dissemination of scientific research documents, whether they are published or not. The documents may come from teaching and research institutions in France or abroad, or from public or private research centers.

L'archive ouverte pluridisciplinaire **HAL**, est destinée au dépôt et à la diffusion de documents scientifiques de niveau recherche, publiés ou non, émanant des établissements d'enseignement et de recherche français ou étrangers, des laboratoires publics ou privés.

Synthesis and magnetic properties of size-selected CoPt nanoparticles

Florent Tournus, Nils Blanc, Alexandre Tamion, Matthias Hillenkamp, Véronique Dupuis

F. Tournus (corresponding author), N. Blanc, A. Tamion, V. Dupuis

LPMCN, Univ. Lyon 1, CNRS UMR 5586, 69622 Villeurbanne, France

Phone: (+33) 472 432 831

Fax: (+33) 472 432 648

e-mail: florent.tournus@univ-lyon1.fr

M. Hillenkamp

LASIM, Univ. Lyon 1, CNRS UMR 5579, 69622 Villeurbanne, France

Abstract

CoPt nanoparticles are widely studied, in particular for their potentially very high magnetic anisotropy. However, their magnetic properties can differ from the bulk ones and they are expected to vary with the particle size. In this paper, we report the synthesis and characterization of well-defined CoPt nanoparticle samples produced in ultrahigh vacuum conditions following a physical route: the mass-selected low energy cluster beam deposition technique. This approach relies on an electrostatic deviation of ionized clusters which allows us to easily adjust the particle size, independently from the deposited equivalent thickness (i.e. the surface or volume particle density in a sample). Diluted samples made of CoPt particles, with different diameters, embedded in amorphous carbon are studied by transmission electron microscopy and superconducting interference device magnetometry. The magnetic anisotropy energy distribution is characterized, showing experimental evidence of a significant anisotropy constant dispersion. We then compare the magnetic properties of two different particle sizes. The results are found to be consistent with an anisotropy constant (including its distribution) which does not evolve with the particle size in the range considered.

Keywords: CoPt alloy, magnetic nanoparticles, size-selected particles, magnetic anisotropy

Introduction

Magnetic nanoparticles have attracted much attention both for their fundamental interest as well as for their potential applications (Hadjipanayis et al. 2008; Xu and Sun 2007; Lu et al 2007). In particular, these nanoparticles might be used for future ultrahigh density magnetic storage devices (Weller et al. 2000). However, below a certain size, the magnetization direction of a particle fluctuates at ambient temperature: the particle is in the superparamagnetic regime. In order to increase the nanomagnets thermal stability, great efforts have been directed toward an enhancement of the nanoparticles magnetic anisotropy (Weller et al. 2000). One of the preferred routes is to use magnetic alloys, and in particular CoPt.

Since the proportion of surface atoms is very large (for instance, 50% of the atoms are at the surface, for a 2.5 nm particle), the properties of magnetic nanoparticles can greatly differ from the bulk ones. Hence, these properties should vary with particle size: a well-defined cluster size distribution is then needed for an accurate investigation. Moreover, in order to “decipher” the size effect, all the other parameters have to be fixed while the particle size is changed. In particular, the particles in a sample must remain far enough from each other to avoid significant magnetic interaction: this is the only way to determine the size-dependent intrinsic magnetic properties. The mass-selected low energy cluster beam deposition technique (MS-LECBD), which is based on laser vaporization followed by ultrahigh vacuum (UHV) deposition of size selected particles, offers such a possibility.

In this paper, we report the synthesis and characterization of well-defined CoPt nanoparticles. After a description of our original synthesis technique, following a physical route, and of the samples studied, we present transmission electron microscopy (TEM) observations and superconducting quantum interference device (SQUID) magnetometry measurements on assemblies of CoPt clusters embedded in amorphous carbon.

Synthesis and structural characterization

CoPt nanoparticles are synthesized using a physical technique, as opposed to chemical synthesis of colloidal particles. We use the low energy cluster beam

deposition (LECBD) technique that allows us to grow thin films of nanoparticles deposited on a substrate (Perez et al. 2001; Perez et al. 2010). We will give a short description of this original technique (see Fig. 1a). Clusters are produced in a laser vaporization-gas condensation source similar to the one developed by Dietz et al. (1981) and Milani and deHeer (1990). Briefly, a plasma created by the impact of a Nd:YAG (yttrium aluminum garnet) laser beam focused on a rod is thermalized by injection of a continuous flow of helium at low pressure typically 30 mbar inducing the clusters growth. Clusters are subsequently stabilized and cooled down in the supersonic expansion taking place at the exit nozzle of the source. A low-energy cluster beam is then obtained, with clusters of different sizes, mostly neutral but also ionized typically 1% of ions.

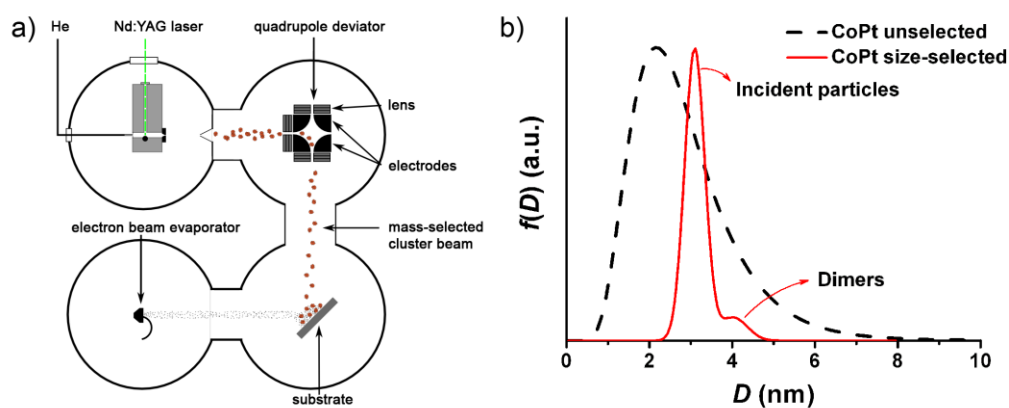


Fig. 1 Schematic view of the MS-LECBD experimental setup (a). Size histogram (deduced from TEM measurements) of size-selected CoPt particles, compared to the case of unselected particles (b)

These ions can be deviated with a quadrupolar electrostatic deflector (described elsewhere) acting as a mass-selection device. In this device (see Fig. 1a), charged clusters (with a charge $q = e$ for single cations) are deviated by application of a selected potential V chosen such as $qV = E_{\text{kinetic}} = 1/2 mv^2$, where m is the clusters' mass and v their velocity. Since previous time-of-flight experiments (Melinon et al. 1995) have revealed that the free clusters' velocity is almost independent of their mass, the energy selection corresponds to a mass selection of the ionized clusters. In addition, the cluster beam is controlled by a set of electrostatic lenses, allowing an optimization of the cluster flux and a good collimation of the beam on the substrate (Alayan et al. 2004). The current

corresponding to the mass-selected ionized cluster beam is then measured by a pico-amperemeter connected to a Faraday cup. This allows us to determine the flux of clusters reaching surface, before deposition on a substrate in UHV conditions: the deposition rate is then fully controlled.

The main key points of this technique are the following. The samples are produced under UHV conditions with a base static pressure of 10^{-10} mbar, and around 10^{-8} mbar during deposition, due to the use of helium as carrier gas. This means that, contrary to other techniques, in particular the chemical synthesis involving ligands, the clusters surface is not altered. Moreover, as shown in Fig. 1a, the samples can be protected by a capping layer in order to avoid any pollution or oxidation when they are exposed to air for subsequent characterizations (Tournus et al. 2008; Tamion et al. 2010). In the present case, we use amorphous carbon as capping layer: it is immiscible with both Co and Pt and enables TEM observations (Tournus et al. 2008). It is important to note that the clusters composition is determined by the one of the target used for laser vaporization. This means that the particles stoichiometry can easily be adjusted by simply changing the target. In the present case, we use an equiatomic CoPt rod, leading to nanoparticles with a composition very close to $\text{Co}_{0.5}\text{Pt}_{0.5}$. Indeed, Rutherford backscattering spectrometry (RBS) experiments indicate that the mean stoichiometry of the clusters films is $\text{Co}_{0.56}\text{Pt}_{0.44}$. Another important feature of the LECBD technique is that the clusters arrive on the substrate in a soft-landing regime, following a random deposition scheme. Consequently, as long as there is no significant diffusion on the substrate, which is the case in this study, the interparticle distance is entirely controlled by the clusters density (the surface density for two-dimensional 2D samples or the volume density for three-dimensional samples where the clusters are embedded in a matrix). This allows us to adjust the strength of interparticle interactions and, by synthesizing highly diluted samples, to obtain thin films of clusters behaving as nearly isolated nanoparticles.

A remarkable feature of the MS-LECBD is the opportunity to change the particle size independently from the interparticle separation: this is not possible in the case of particles grown by atomic deposition on a surface. The efficiency of the mass selection device can be seen in Fig. 1b where cluster size distributions with and without selection are compared. The relative size dispersion is reduced

by a factor of 6, down to $\sigma_D/D_m \sim 7-8\%$ where σ_D and D_m are respectively the standard deviation and the median diameter of the Gaussian distribution that fits the incident particle size. A small shoulder can be seen in Fig. 1b, which is due to the low proportion of dimers (two particles partially coalesced) formed on the substrate, simply because of the random nature of cluster deposition. Remarkably, this proportion ($\sim 8\%$) is indeed in excellent agreement with the value expected just from the probability (which is fixed by the density and the cluster size) for a cluster to land on another one already lying on the surface: this means that incident clusters do not diffuse on the amorphous carbon film.

Our experimental setup can be used to produce particles with a diameter in the range 1 to 5 nm (Tainoff et al. 2008). The cluster size is easily controlled by choosing the deviation potential V , as illustrated in Fig. 2. Note that the relative size dispersion does not depend on V , and consequently on the cluster size. However, for the largest particles a shape distribution is visible.

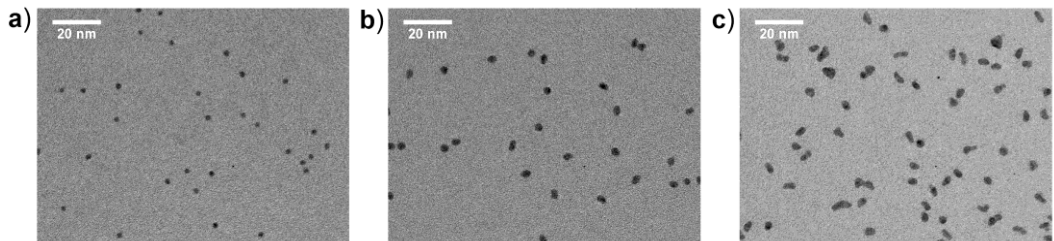


Fig. 2 TEM images of size-selected CoPt clusters deposited on an amorphous carbon film and capped with an amorphous carbon layer. The deviation potential is 100 V (a), 300 V (b) and 500 V (c) corresponding respectively to a median diameter of $D_m = 2.0$ nm, $D_m = 3.1$ nm and $D_m = 3.8$ nm.

Magnetometry measurements

Thin films of CoPt cluster layers (0.5 \AA equivalent thickness per layer) separated by 5 nm of carbon matrix has been synthesized by the MS-LECBD technique described above. The samples' dilution (1 vol %) ensures that the interparticle magnetic interactions are negligible: the mean first-neighbor distance is around 7 nm. The clusters size distribution is either the one represented in Fig. 1b with $D_m = 3.1$ nm, corresponding to a 300 V deviation potential, or the similar one, centered on $D_m = 3.8$ nm, corresponding to a 500 V deviation potential. As expected, the as prepared CoPt particles are crystallized in the chemically

disordered A1 face-centered-cubic phase (Tournus et al. 2008). Superconducting quantum interference device (SQUID) magnetometry (Quantum Design MPMS magnetometer) is used to characterize the magnetic properties of the embedded clusters, from low-field susceptibility measurements ZFC/FC protocol, with a 50 Oe magnetic field and hysteresis loops at various temperatures.

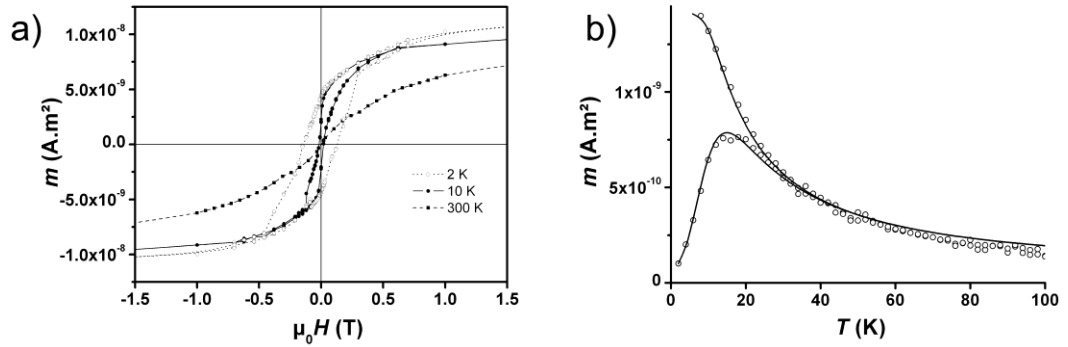


Fig. 3 Hysteresis loops at 2 K, 10 K and 300 K (a) ZFC/FC susceptibility curves (b) for 3.1 nm CoPt particles. Data points correspond to experimental measurements and the lines are either a guide to the eyes (a) or a theoretical fit (b)

The magnetic curves obtained for the 3.1 nm particles sample are shown in Fig. 3. The remnant to saturation ratio of the magnetization at 2 K is fully consistent with the model of non-interacting and randomly oriented uniaxial macrospins (Stoner-Wohlfarth model), i.e. it is less than 0.5 (Stoner and Wohlfarth 1948). We also observe the expected $1/T$ scaling both for the susceptibility curves and the magnetization loops, as long as the temperature is high enough for the system to be in the superparamagnetic regime. Moreover, we have verified that the magnetic measurements are identical with in-plane or perpendicular applied magnetic field, which means that interparticle interactions are safely negligible.

The coercive field is reduced from 1400 to 180 Oe when the temperature goes from 2 to 10 K because some particles have become superparamagnetic: the 10 K magnetization loop has the characteristic “wasp waist” shape corresponding to the superposition of a blocked contribution and a superparamagnetic one. For higher temperatures, the system is completely superparamagnetic and the $m(H)$ curve at room temperature can be successfully adjusted by a Langevin function using the size distribution deduced from TEM measurements. This is in agreement with previous observations on unselected CoPt clusters (Tournus et al. 2008),

where the amorphous carbon matrix was shown to preserve the magnetic cluster size: $D_{\text{mag}} = D_{\text{TEM}}$, i.e. there is no magnetically dead layer.

In order to characterize the particles magnetic anisotropy, we try to simultaneously adjust the ZFC/FC curves and the high-temperature magnetization loop (300 K) with a semi-analytical theoretical model, following the “triple-fit” procedure recently described (Tamion et al. 2009). Whereas a single anisotropy constant K_{eff} (the anisotropy energy of a particle of volume V is then $E_{\text{ani}} = K_{\text{eff}} V$) does not allow to fit the curves (Tournus et al. 2010), we find that a Gaussian dispersion of K_{eff} can successfully account for the three curves, while keeping the TEM particles’ size distribution. A best fit provides the value of the mean anisotropy constant $K_0 = 218 \text{ kJ/m}^3$ and the relative K_{eff} dispersion $w_K = \sigma_K/K_0 = 37\%$, with σ_K the standard deviation. Interestingly, the mean anisotropy constant is consistent with the value of K_{eff} previously reported for unselected CoPt clusters. Following the theoretical considerations of Tournus, Rohart and Dupuis (2008), we can attribute the K_{eff} dispersion mainly to the multiplicity of atomic configurations: a huge number of chemical arrangements can indeed statistically exist in the case of chemically disordered particles of the same geometry size and shape, corresponding to different values of E_{ani} and hence K_{eff} .

The magnetic curves obtained for the sample of 3.8 nm diameter particles are shown in Fig. 4. As for the 3.1 nm diameter particles, the coercive field decreases when the temperature increases. According to the Stoner-Wohlfarth model, the coercive field H_C at 0 K does not explicitly depend on the particle size. It is directly linked to the anisotropy field: $H_C = 0.49 H_{\text{ani}} = 0.49 \times 2 K_{\text{eff}}/(\mu_0 M_S)$, with M_S the saturation magnetization of the particles (which must be independent of the size). Nevertheless, the measured H_C for two distinct particle sizes could differ for two reasons: first, because of a size effect on the anisotropy constant (a K_{eff} evolution with V); second, because in fact the measurements are not performed at 0 K. If the temperature is not strictly zero, the particle size distribution in the sample can indeed significantly change H_C . In the present case, we find very similar value of H_C for the two samples at 2 K. Assuming that a 2 K temperature is low enough to extrapolate this result to 0 K, this crude approach tends to show that the anisotropy constant is almost the same for the two particle sizes.

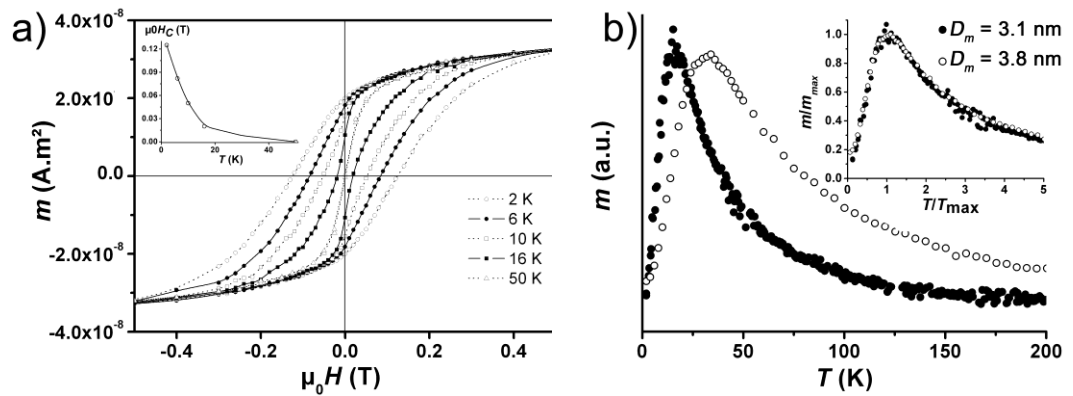


Fig. 4 Hysteresis loops at 2 K, 6 K, 10 K, 16 K and 50 K for 3.8 nm CoPt particles (a). The coercive field evolution is given in insert. The lines are just guides to the eyes, data points corresponding to experimental measurements. Experimental ZFC susceptibility curves for 3.8 nm CoPt particles compared to the 3.1 nm particles (b). Normalized curves are shown in insert.

Besides, compared to the sample of 3.1 nm diameter particles, the “wasp waist” shape is much less pronounced at 10 K for the 3.8 nm diameter particles. This indicates that the contribution of particles in the superparamagnetic regime is weaker: the blocking temperature should then be higher for the 3.8 nm diameter particles than for the 3.1 nm ones. This is exactly what can be seen in Fig. 4b where the ZFC curves of the two samples are compared: the susceptibility peak is situated at $T_{\max} = 32$ K for the 3.8 nm diameter particles, while we have $T_{\max} = 17$ K for the 3.1 nm diameter particles. In fact, the T_{\max} increase can be explained by a direct size effect: the ZFC shape is determined by the E_{ani} distribution (which scales linearly with the particle volume) and we find that the 1.88 ratio between the two T_{\max} values is fully consistent with the 1.84 ratio between the two particles volume. Moreover, we can consider the entire ZFC curves (not only the ZFC peak at T_{\max}), and compare the normalized curves (see Fig. 4b insert). We find that the ZFC evolution with the particle size is only due to a simple scale effect: the size distribution has the same shape and the anisotropy constant (including its dispersion, as discussed above) is the same for the two diameters.

Conclusion

We have demonstrated that the MS-LECBD technique can successfully produce high quality samples made of well-defined clusters embedded in a matrix, with a controlled dilution. This original approach offers a quite unique

opportunity to vary *independently* the particle size and the interparticle separation. In this way, model samples have been synthesized: the interparticle interactions are negligible, the particle environment is controlled (UHV deposition, followed by an amorphous carbon capping), and the particle size distribution is narrow and perfectly known. The intrinsic properties of the nanoparticles can then be determined which opens the way to an accurate size effect investigation.

Magnetic measurements on size-selected particles with a diameter around 3 nm have evidenced an anisotropy constant dispersion. Small particles with a well-defined size are needed to make this effect visible: a K_{eff} distribution cannot be detected for unselected particles assemblies.

We have compared the magnetic measurements on two samples made of different particle sizes: 3.1 nm diameter particles and larger particles of 3.8 nm diameter, which nearly corresponds to twice the number of atoms. The results are consistent with an anisotropy constant (including its distribution) which does not evolve with the particle size. The different magnetic behaviour can be explained only by a direct size effect on the magnetization switching energy barrier. Therefore, by tailoring the particle size (i.e. simply choosing the deviation potential), some useful magnetic properties, in particular the blocking temperature, can be easily adjusted.

Acknowledgement The authors gratefully acknowledge O. Boisron, and the Centre de Magnétométrie de Lyon (CML).

References

Alayan R et al (2004) Application of a static quadrupole deviator to the deposition of size-selected cluster ions from a laser vaporization source. *Rev. Sci. Instrum.* 75:2461

Dietz TG, Duncan MA, Powers DE, Smalley RE (1981) Laser production of supersonic metal cluster beams. *J. Chem. Phys.* 74:6511

Hadjipanayis CG et al (2008) Metallic Iron Nanoparticles for MRI Contrast Enhancement and Local Hyperthermia. *Small* 4:1925

Lu AH, Salabas EL, Schüth F (2007) Magnetic Nanoparticles: Synthesis, Protection, Functionalization, and Application. *Angew. Chem., Int. Ed.* 46:1222

- Melinon P et al (1995) From free clusters to cluster-assembled materials. *Int. J. Mod. Phys. B* 9:339
- Milani P, deHeer WA (1990) Improved pulsed laser vaporization source for production of intense beams of neutral and ionized clusters. *Rev. Sci. Instr.* 61:1835
- Perez A et al (2001) Nanostructured Materials from Clusters: Synthesis and Properties. *Mater. Trans.* 42:1460
- Perez A et al (2010) Functional nanostructures from clusters. *Int. J. Nanotechnol.* 7:523
- Stoner EC, Wohlfarth EP (1948) A mechanism of magnetic hysteresis in heterogeneous alloys. *Phil. Trans. R. Soc. Lond. A* 240:599
- Tainoff D et al (2008) Self-Organization of Size-Selected Bare Platinum Nanoclusters: Toward Ultra-dense Catalytic Systems. *J. Phys. Chem. C* 112:6842
- Tamion A, Hillenkamp M, Tournus F, Bonet E, Dupuis V (2009) Accurate determination of the magnetic anisotropy in cluster-assembled nanostructures. *Appl. Phys. Lett.* 95:062503
- Tamion A et al (2010) Magnetic anisotropy of embedded Co nanoparticles: Influence of the surrounding matrix. *Phys. Rev. B* 81:144403
- Tournus F et al (2008) Evidence of L10 chemical order in CoPt nanoclusters: Direct observation and magnetic signature. *Phys. Rev. B* 77:144411
- Tournus F et al (2008) XMCD study of CoPt nanoparticles embedded in MgO and amorphous carbon matrices. *J. Electr. Spectr. Relat. Phenom.* 166–167:84
- Tournus F, Rohart S, Dupuis V (2008) Magnetic Anisotropy Dispersion in CoPt Nanoparticles: An Evaluation Using the Néel Model. *IEEE Trans. Magn.* 44:3201
- Tournus F, Blanc N, Tamion A, Hillenkamp M, Dupuis V (2010) Dispersion of magnetic anisotropy in size-selected CoPt clusters. *Phys. Rev. B* 81:220405(R)
- Weller D et al (2000) High Ku materials approach to 100 Gbits/in². *IEEE Trans. Magn.* 36:10
- Xu C, Sun S (2007) Monodisperse magnetic nanoparticles for biomedical applications. *Polym. Int.* 56:821